Seasonal variability of stream water quality response to storm events captured using high-frequency and multi-parameter data

Ophélie Fovet, G. Humbert, Rémi Dupas, Chantal Gascuel, Gérard Gruau, Anne Jaffrézic, G. Thelusma, M. Faucheux, N. Gilliet, Y. Hamon, et al.

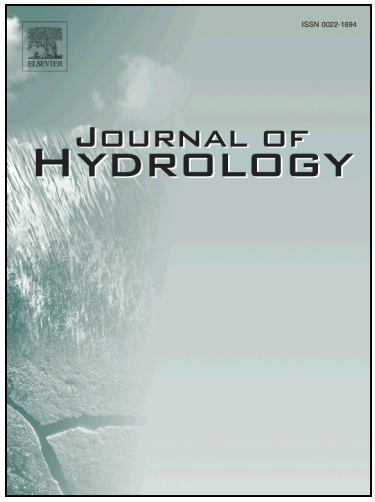

Research papers

Seasonal variability of stream water quality response to storm events captured using high-frequency and multi-parameter data

O. Fovet, G. Humbert, R. Dupas, C. Gascuel-Odoux, G. Gruau, A. Jaffrezic, G. Thelusma, M. Faucheux, N. Gilliet, Y. Hamon, C. Grimaldi

PII: S0022-1694(18)30117-3
DOI: https://doi.org/10.1016/j.jhydrol.2018.02.040
Reference: HYDROL 22589

To appear in: *Journal of Hydrology*

Received Date: 12 July 2017
Revised Date: 3 January 2018
Accepted Date: 14 February 2018

Please cite this article as: Fovet, O., Humbert, G., Dupas, R., Gascuel-Odoux, C., Gruau, G., Jaffrezic, A., Thelusma, G., Faucheux, M., Gilliet, N., Hamon, Y., Grimaldi, C., Seasonal variability of stream water quality response to storm events captured using high-frequency and multi-parameter data, *Journal of Hydrology* (2018), doi: https://doi.org/10.1016/j.jhydrol.2018.02.040

Seasonal variability of stream water quality response to storm events captured using high-frequency and multi-parameter data

O. Fovet[1], G. Humbert[1], R. Dupas [1], C. Gascuel-Odoux[1], G. Gruau[2], A. Jaffrezic[1] , G. Thelusma[1], M. Faucheux[1], N. Gilliet[1], Y. Hamon[1], and C. Grimaldi[1]

[1]UMR SAS, INRA, AGROCAMPUS OUEST, 65 rue de Saint Brieuc, 35042 Rennes, France

[2]Observatoire des Sciences de l'Univers de Rennes, CNRS, UMR 6118 Géosciences Rennes, Campus de Beaulieu, Rennes, France)

Corresponding author: Ophelie Fovet (ophelie.fovet@inra.fr; +33 223 485 438)

Abstract

The response of stream chemistry to storm is of major interest for understanding the export of dissolved and particulate species from catchments. The related challenge is the identification of active hydrological flow paths during these events and of the sources of chemical elements for which these events are hot moments of exports. An original four-year data set that combines high frequency records of stream flow, turbidity, nitrate and dissolved organic carbon concentrations, and piezometric levels was used to characterize storm responses in a headwater agricultural catchment. The data set was used to test to which extend the shallow groundwater was impacting the variability of storm responses. A total of 177 events were described using a set of quantitative and functional descriptors related to precipitation, stream and groundwater pre-event status and event dynamics, and to the relative dynamics between water quality parameters and flow via hysteresis indices. This approach led to identify different types of response for each water quality parameter which occurrence can be quantified and related to the seasonal functioning of the catchment. This study demonstrates that high-frequency records of water quality are precious tools to study /unique in their ability to emphasize the variability of catchment storm responses.

1 Introduction

Stream hydro-chemical dynamics during storm events are a major topic of investigation to understand and predict catchments export regimes of chemical elements of major interest such as Dissolved Organic Carbon (DOC, e.g. McGlynn and McDonnell, 2003) or Phosphorus (P, e.g. Bowes et al., 2005). The reasons of this interest are that storms export the major part of the annual flux and they are critical moments of connections between element sources and stream and thus for element exports too (Vidon et al., 2010).

The ephemeral nature of such events make them difficult to monitor so that only a few storm studies have been interested in more than 1 parameter (Hill, 1993; Ladouche et al., 2001; Ockenden et al., 2016), with most using a limited number (<10) of storms (Bernal et al., 2002; Borah and Bera, 2004; Inamdar and Mitchell, 2006).

Such constraints are now relaxed thanks to the development of nearly-continuous monitoring techniques (Kirchner et al., 2004; Ockenden et al., 2016; Rode et al., 2016; van Geer et al., 2016; Blaen et al., 2016; Ruhala and Zarnetske, 2017) that enable the measurements of non-hydrological parameters such as turbidity (Lawler et al., 2006), electrical conductivity (Penna et al., 2015), or concentrations of Nitrate (NO_3) or mineral Nitrogen (N), Dissolved or Total Organic Carbon (TOC), Total Suspended Solids (TSS), and Phosphorus (P) (Jordan et al., 2007; Halliday et al., 2013; Bowes et al., 2015; Jeong et al., 2012; Lloyd et al., 2016; Ockenden et al., 2016, Feinson et al., 2016, Sherriff et al., 2016).

At high temporal frequencies, it is possible to analyze the relative variations of chemical variables with flow (Q), highlighting particular relationships such as hystereses (Bowes et al., 2005; Lefrancois et al., 2007; Jiang et al., 2010; Wade et al., 2012; Cerro et al., 2014; Bieroza and Heathwaite, 2015). Such relationships express lag times between discharge and chemical variations to identify sources and flow paths. With the continuity of the monitoring, the number of recorded events increased allowing for the analysis of their variability. Several investigations have been conducted using multivariate statistics to assess the role of various hydrological and meteorological variables or catchment features (size, topography, soil types, land use) (Bernal et al., 2002; McGlynn and McDonnell, 2003; Lloyd et al., 2016; Sherriff et al., 2016; Feinson et al., 2016).

The seasonal variability of stream water composition has been mainly studied for base flow but much less for storm flow. Feinson et al. (2016) found that seasonal effect on storm NO_3-Q hystereses was site specific. Sherriff et al. (2016) related the variations in TSS-Q storm

patterns to the combination of seasonal changes in connectivity and in source availability depending on catchment permeability and seasonal land cover variability (arable vs grasslands). Outram et al. (2016) found that groundwater depth and runoff coefficients were impacting the NO3 exports via activation of sub-surface pathways and tile drain flow while Phosphorus exports were affected by antecedence of dry conditions and depicted exhaustion with time because of depletion via temporarily connection of surface pathways.

In crystalline bedrock, the role of shallow groundwater in base flow hydrochemistry has been well demonstrated (Molenat et al., 2008; Gascuel-Odoux et al., 2010; Lambert et al., 2013; Aubert et al., 2013a). The succession of hydrological seasons has not been yet tested for storm flow events but is assumed to play a role by modifying element sources mobilized during storm as well via changes in catchment connectivity. Some attempts have been done on daily data, using qualitative storm patterns (Aubert et al., 2013c), or on Phosphorus concentration using a partial storm data set of 8 events per year (Dupas et al., 2015a). But the moderate number of storm events or parameters analyzed as well the daily time step limit any storm typology.

To test our hypothesis that in catchments dominated by subsurface flows, shallow groundwater was directly structuring the temporal variability of storm events, we explore the seasonal changes in storm responses using continuous high frequency data set of multiple parameters. To characterize this temporal variability of storm responses we proposed a method adapted to such data set. The records included stream flow, turbidity and concentrations in DOC and NO_3, and piezometric levels from a small agricultural catchment over up to 177 storm events over 4 water years. The method consisted in

(i) identifying a set of functional indicators, based among a large set of descriptors of precipitation input, antecedent and initial discharge and groundwater conditions, and of combined hydro/chemical responses.

(ii) analyzing the controlling factors of intra-annual variations of chemical storm responses, in particular the role of shallow groundwater in determining the hydro-chemical connectivity within the catchment.

2 Material and Method

2.1 Study site and season delineation

The headwater catchment of Kervidy-Naizin is part of the long-term Environmental Research Observatory AgrHyS (http://www6.inra.fr/ore_agrhys_eng/) which supports research on response times of agricultural catchments with regard to hydrological and biogeochemical fluxes since 1993 and which is part of the French "Observatories of Critical Zone, Applications and Research" (OZCAR) since 2017. The 5 km^2 and 2^{nd} Strahler order catchment is located in Brittany, Western France (see Fig 1), and characterized by gentle slopes (<5%), loamy and loamy-sandy soils varying from 0.3 to 1 m deep with 3 domains : poorly drained soils in the bottom lands, moderately well drained soils in the midslope areas and well drained soils in the upland areas. The bedrock is dominated by schist with a weathered zone from 1 m to 30 m deep. The climate is temperate and humid with annual precipitation of 853 mm (+/- 210 mm) occurring only as rainfall, annual runoff of 340 mm (+/- 169 mm) and Penman Potential Evapotranspiration of 697 mm (+/- 57 mm) in average over the period 2000-2016. Landscape is dominated by agriculture with crop-farming systems including mostly indoors pig and dairy farming and the area is covered by cereals and rapeseeds (about 30%), grassland (about 30%) and maize (about 30%), a map of the land cover is provided in Fig S7.

The seasonal variability in the catchment has been mainly studied and well characterized for base flow regarding hydrology and water chemical composition (Aubert et al., 2013a; Aubert et al., 2013b; Humbert et al., 2015; Lambert et al., 2013; Molenat et al., 2002). From these

works a conceptual model has been built for the catchment that is based on an annual cycle of 4 hydrological periods more or less consistent with the temperate calendar seasons because they are defined according to piezometric variations and meteorological conditions (see details in Humbert et al. (2015). In brief, these 4 periods are related to the dynamics of water catchment storage: the rewetting phase (from late summer to winter), the high flow period (autumn to early spring), the recession phase (late winter to summer) and the drought (summer to autumn).

2.2 Data acquisition

Time series used in this study extended from September 2010 to August 2014, hydro-meteorological variables were recorded for longer periods thus comparison of their values between the study period and the whole period are provided in SI (Fig S2a and Fig S3).

Hourly precipitations were recorded at the weather station (located just outside the catchment, see Fig 1) in a tipping bucket rain gauge (Cimel Enerco 516i). Stream flow was calculated using a rating curve and measured stream levels at the Kervidy station (Fig 1) thanks to a pressure transducer Thalimedes OTT recording at 1min time step. Shallow groundwater levels were measured in the 5 piezometers denoted PKu/d and PGu/m/d (for upslope, midslope and downslope locations respectively) in Fig 1 thanks to pressure sensors Orpheus Mini OTT recording at 15min time step. All these automatic records are regularly checked with manual measurements (monthly for rainfall, every 2-3 months for piezometers) or an additional sensor (an Orpheus Mini OTT as well for stream flow).

Turbidity was measured directly in the stream at the Kervidy station using a PONSE TU-NA probe with a 10 min time step and expressed as Formazine Turbidity Unit (FTU). The probe was cleaned manually every 1 to 2 weeks by brushing it in addition to an automatic scraping system. As the stream dries out every summer for a few weeks, the probe is yearly fully

cleaned and recalibrated in the laboratory, using a formazine solution and replaced in the stream during the early fall. The turbidity is deduced from the measurement of optical absorbance in infrared (880 nm).

DOC and NO_3 concentrations were measured in situ at the Kervidy station using an indirect method based on absorbance measurement in UV and visible thanks to a spectrolyser S:CAN with a 15 to 20 min time step. The concentration values were obtained from absorbance measurements every 2.5 nm from 200 to 740 nm after turbidity automatic compensation and using a Partial Least Square Regression equation provided by the manufacturer. These concentrations values were then locally recalibrated using a set of manually grabbed samples filtered at 0.2 µm and analyzed for NO_3 and DOC concentrations in the laboratory (by ionic chromatography for nitrate and by thermic oxidation and Infra-Red detection for DOC). This data set included stream water sampled both during base flow and storm flow conditions. The storm event samples were obtained using an automatic ISCO sampler for a few storms along the year. Local recalibrations have been performed once for NO_3 and year by year for DOC as it appeared to be the best option probably because the stream dries out every summer for a few weeks when the spectrolyser is removed for being fully cleaned at laboratory (Faucheux and Fovet, 2014). Finally, the local recalibration used 66 to 120 points (66 to 120 points depending on the year for DOC, and once with 120 points for NO_3). Comparison between continuous records and manual sampling of these concentrations are provided in supplementary material. Such calibration led to a mean error between spectrolyser and laboratory concentration values of ±0.6 mg DOC/L (median base flow value: 6.1 mg/L) and of ±0.74 mg NO_3/L (median base flow value: 62.6 mg/L). The spectrolyser was auto-cleaned by compressed air before each measurement and manually brushed every 1 or 2 weeks. However, it was not sufficient to avoid biofouling of the probe especially when light conditions were optimal for biofilms. Nitrate concentrations were not sensitive to this

biofouling whereas DOC concentrations were obviously disturbed. This led us to disregard some periods (from February usually) of DOC measurement in the analysis in order to insure the reliability of the data. In total, despite sensor failures and the drift issue for DOC: Turbidity, NO_3 and DOC data were available for 86%, 84% and 42% of the storm events respectively. Time series are provided in Supplementary material (SI Fig S1),

2.3 Storm event identification and delimitation

Stream flow time series was resampled from a 1 min time step to a 10 min time step. Storm event detection was based on the flow variations, and then controlled by previous precipitations as performed similarly in previous studies of storm events on this catchment (Aubert et al., 2013c; Dupas et al., 2015a; Dupas et al., 2015c; Humbert et al., 2015). If the variation of instantaneous flow in 10 min was greater than 2 L/s, and if precipitations cumulated over preceding 24h was greater or equal to 5 mm, then a storm event was identified at the corresponding date. The end of the storm was either the time when stream flow recovered its initial value or if it remained higher than this initial value because of the persistence of wet conditions, it was chosen as the time when stream flow was minimal after the peak flow and before the next event. Some of the selected events were thus consistently exhibiting multiple peaks. The storm identification has been performed on Scilab©.

Figure 1. Map of the study site and location of monitoring stations

2.4 Set of storm descriptors

For each storm, the 10 min instantaneous stream flow time series were used to identify initial, final, minimal and maximal values of stream flow and their corresponding times. Then, the raw data of turbidity (Tu), piezometric records (Gu,d and Ku,m,d), and NO_3 and DOC concentration records were used to identify also initial (Xi), final (Xf), minimal and maximal

values for each of those variables and their corresponding times. On the hourly precipitation data, we computed the cumulated rainfall amount for the 24h preceding the initial time of the storm (P_{-24h}), and the amount of rainfall cumulated between 6h before the initial time and the time corresponding to maximal stream flow as an estimate of event precipitation amount (P_{ev}), and the Antecedent Precipitation Index over 4 days (API). Longer periods have been tested for API and appeared less relevant because the stream reacts to short and small rain events thus to events that are occurring close together. The duration of the rising phase (ΔT_{ris}) was the difference between flow peak time and initial times. For each variable X, we computed the variation ΔX as the difference between maximal and initial value or between minimal and initial value of X, if higher in terms of absolute value.

As the intensity of each variable response was described by ΔX, we normalized the flow, turbidity and concentrations between 0 and 1 for each event in order to allow comparing storms with each other. For each storm, $X^*=1$ corresponding the maximal value of X and $X^*=0$ corresponding to the minimal one and between both, the transformation was linear (Lloyd et al., 2015; Butturini et al., 2008).

Then best linear regression between Q^* and NO_3^*, DOC^* or Tu^* was fitted, and described using the value of the slope α, of the determination coefficient R^2, and of the slope using only the points in the rising phase of the storm (α_{ris}). To characterize properly the hysteresis when it occurred, we also calculated a set of Hysteresis Indices denoted HI proposed by Lloyd et al. (2015) and slightly modified from Lawler et al. (2006):

$$HI_k = X_R^*(Q^* = k) - X_F^*(Q^* = k)$$

With X^*_R and X^*_F being the value of X^* for which $Q^*=k$ in the rising and falling phases respectively. We used 3 values for k: 0.25, 0.5 and 0.75 as an attempt to integrate the whole loop in the description as suggested by (Lloyd et al., 2015) in order to avoid misinterpretation when the hysteretic loop is restricted around high or low values (and thus not detectable at

50% of Q range). Hysteresis pattern have been widely studied for describing storm event dynamics, and there are a few quantitative descriptors of these patterns that have been proposed (House and Warwick, 1998; Johnson and East, 1982; Lawler et al., 2006; Butturini et al., 2008; Cerro et al., 2014; Lloyd et al., 2015; Dupas et al., 2015a; Feinson et al., 2016). Some models also have been proposed to reproduce such relationships (Bowes et al., 2005). Among the possible descriptors, they are all interested in describing similar main features: the direction of the loop, the elongation or the width of the loop, and its slope.

- The direction of the loop can be deduced from the sign the Hysteresis Index above. Using 3 values of HI allowed us to describe the direction even for non-simple loop. Positive values indicate clockwise direction while negative values anticlockwise rotation.
- The slope of the hysteresis is given by the slopes of the fitted relationship between normalized turbidity or concentration and normalized flow (α and α_{ris}). Positive values indicate accretion patterns and negative values dilution patterns.
- The width of the hysteresis could be partly described by the determination coefficient R^2 and by the absolute value of HI_k that is equal to 0 when the relationship is not hysteretic and tends to increase when falling limb concentrations digress from rising limb concentrations for each discharge value.

Descriptors have been calculated using Scilab© (Scilab Enterprises, 2012), and statistics calculations and correlation analyses performed on the descriptors set have been conducted using R© (R Development Core Team , 2008).

3 Results

3.1 Inter-annual variability of the hydroclimate depicted in the data set

The hydroclimatic features of each year of the data series compared to their ranges over the period 2000-2016 in order to characterize the 4 studied years in a larger picture of the

catchment are provided in SI (Figs S2, S3). The year 2013-2014 is particularly wet with higher total runoff and definitively more numerous storm events (83 versus 29 to 33 for the first 3 years). The studied 4 year period is thus composed of both standard and extreme years in terms of water flux, piezometric levels, and storm occurrence. The seasonal hydrological periods defined as described in the Material and Method section divide the water year in functional phases that revealed the variability of these phases from a year to another. The median duration of rewetting, high flow and recession periods were 49, 123 and 65 days respectively with a standard deviation of 54, 29 and 48 days respectively over the period 2000-2014. The distribution of storm events in the data set between each hydrological period is not uniform because of the difference in their duration and the obvious higher occurrence of storms in the high flow period. The turbidity and NO_3 data sets count 145 storms with 4% of them occurring during the rewetting period, 80% during the high flow period and 16% during the recession period. Because of the drift issue on DOC data, the corresponding time series count only 71 storms (Table 1, raw "*n*") with 8% of them occurring during the rewetting periods, 92% during the high flow period, and no exploitable storm during the recession period.

3.2 Average storm events characteristics

Tables 1 to 3 summarized the general statistics obtained for each descriptive variable. Antecedent precipitations over 24h that generate a storm are in average about 6.1 mm. Initial stream flow ranged between 0 and more than 300 L/s. Initial groundwater in the downslope riparian area (Kd, Gd) was up to 2.3 m below ground surface but less than 20 cm deep for 75% of time while in the upland hillslope (Ku, Gu) water table was deeper (up to 5 m deep in Gu, less than 2 m deep for 75% of time, Table1). Initial turbidity was usually low (less than 20 FTU), initial NO_3 and DOC concentrations ranged from 17.8 to 78.5 and from 2.5 to 15.5

respectively (Table 1). The variation of stream flow during the storm was highly variable: in average 161 L/s ±225 L/s. Groundwater was reactive to storm events depending of the slope position, with a median variation of water table during storms between 4 and 5 cm for all piezometers and ranging from 0 to 1.7 m (Table 2).

3.3 Dominant hysteretic patterns

Turbidity exhibited an accretion pattern during storm: both ΔTu (194±334 FTU in average and 73 FTU in median value) and the slopes of Turbidity-Flow relationship were positive (Tables 2 and 3). The determination coefficient of a linear regression between Tu and Q (R^2 Tu) was usually poor (0.5 in average). The Turbidity-Flow usually exhibits a hysteresis with systematically different slopes for whole event (0.5) and the rising limb only (0.55). The loop was usually positive (accretion pattern) and clockwise as indicated by overall positive values of Hysteresis indices HI_{Tu} (0.18, 0.27 and 0.32 in average for 25, 50 and 75 % of maximal flow respectively) as reported in Table 3. This accretion pattern represented 100% of the analyzed events and the clockwise hysteresis 92 to 100% (according to $HI_{Tu}(75)$ and $HI_{Tu}(50)$ respectively) of the events.

Nitrate concentration exhibited a dilution pattern during storm: ΔNO_3 (about -17 mg of NO_3/l in average, Table 2), the slopes of linear regression between [NO_3] and Q were negative for more than 90% of the events (Table 3). The [NO_3]-Flow dynamics seemed more linear but still slightly hysteretic. Indeed, determination coefficients of the linear regressions were usually greater than 0.5 (about 0.76 in average) and the HI absolute values were smaller than for the other chemical proxies (Table 3). Median values of the descriptors indicated that the loop was negative (dilution pattern) and clockwise as indicated by positive average and median HI_N values and by the slopes of linear regression between concentration and flow (α

NO_3<α_{ris} NO_3<0). The dilution pattern represented 98% of the analyzed events and the clockwise hysteresis 76 to 78% (for $HI_N(75)$ and $HI_N(50)$ respectively) of the events.

DOC concentration exhibited an accretion pattern during storm as Turbidity with average amplitude (ΔDOC) of 5 mg C/l ±4 (Table 2). The slopes of the linear regression between DOC concentration and discharge were also both positives (Table 3). The [DOC]-flow relationship was hysteretic with HI_C absolute values similar to those of HI_{Tu} (between 0.1 and 0.3 in median and average) and rather poor linear regressions (R^2 for DOC about 0.55 in average). The hysteretic loops were dominantly positive (accretion pattern) and anticlockwise as expressed by negative average and median HI_C values and higher values of α comparing to α_{ris} for the [DOC]-Q linear regressions (Table 3). The accretion pattern represented 92% of the analyzed events and the anticlockwise hysteresis 90 to 92% (for $HI_C(75)$ and $HI_C(50)$ respectively) of the events.

3.3 Correlations between descriptor variables

Pearson correlation coefficients between descriptors are provided in SI (Tables S2 to S4). Significant correlations were logically found between the groundwater depths, and between flow variables and groundwater depths. The amplitude of flow variation was correlated to the event precipitation (Pearson coefficient is 0.5) and poorly but significantly to groundwater levels, while the duration of rising limb was only significantly correlated to the event precipitation (Table S2).

Initial turbidity was positively and significantly correlated to initial and antecedent conditions, and the amplitude of turbidity response with event precipitation and flow amplitude. The turbidity-flow hysteresis indices were positively correlated to groundwater levels and flow variables (Table S3, S4).

The amplitude of nitrate concentration was negatively correlated to the variation of flow, and highest significant correlations for the NO_3-variables were between determination coefficient R^2 for NO_3 and initial groundwater levels (Tables S3, S4).

Initial DOC concentration was positively and significantly correlated to antecedent conditions, and the amplitude of DOC response was negatively correlated to the hydrological variables (initial flow and groundwater levels) and positively to the event duration and precipitation (ΔTris and Pev). The slope of DOC-Q linear regression was related to initial flow and downslope groundwater depth by negative correlation. The DOC-flow hysteresis indices were significantly but poorly correlated with the event duration (ΔTris, Tables S3, S4).

3.4 Variability of stream response to storm events with season

The variations of storm response descriptors have been analyzed according to hydrological periods defined on effective groundwater variations and meteorological variables. For a detailed view of intra-annual variability, the results on monthly variations are also provided in SI (Figs S4, S5). The variations of hydrological variables describing the storm response were relatively moderated (Fig 2) and very similar to the intra-annual variations of groundwater (Fig 2e,f). Base flow is fed mainly by this groundwater variations controlled by the difference between precipitations and evapotranspiration (Aubert et al., 2013b). In the rewetting phase at the beginning of the water year (end of Summer-early Fall), the catchment storage was minimal so that highest rain was required for an event to occur leading to highest values of API and event precipitation (Fig 2a,b). On the contrary, during the winter high flow period, catchment storage was maximal, so that smaller precipitation events were sufficient to generate higher runoff responses (Pev lowest and ΔQ highest, Fig 2a,b,c). At the recession and low flow periods (Spring to Summer), the storage was decreasing leading to lower

catchment reactivity leading to shorter storms (Fig 2d) occurring in potentially drier conditions (Fig 2b).

The intra-annual variations of hydrochemical responses to storm event in the stream were specific to each parameter. The amplitude of turbidity variations was generally higher during the high flow period but also highly variable during the recession phase (Fig 3a) likely to reach really high values. The values of HI_{Tu} were increasing in the winter period of high flow (Fig 3g). Fig 3d showed a seasonal increase of the slopes of Tu-Q relationship after the rewetting phase.

The slopes of linear regression between NO_3 concentration and flow (Fig 3e) during the high flow period were more negative and closer to each other (comparing slopes computed on the whole event data or on the rising limb phase only) than in the dry periods (rewetting and recession). The difference between the 2 slopes (whole event vs. rising limb only) was indeed higher for the recession period (Fig 3e). The HI_N values were also more variable with higher maxima during these drier periods (Fig 3h).

Due to drift issues of the DOC indirect absorbance measurements, we were able to use data from storm event that occurred only during the first part of the water year. Thus, no DOC descriptors could have been used for the recession period. However, over this wet periods, both the amplitude of DOC variation (Fig 3c) and slopes of the linear regression between DOC concentration and flow (Fig 3f) seemed to decrease continuously over the water year (SI Fig S5). No trend appeared on the HI_C variation (Fig 3i).

For several descriptors, the higher variability of the descriptors in rewetting period expresses the occurrence of values in break with the trend over following months at the very start of the water year (usually October). For instance, HI_{Tu} (SI Fig S5g) were high compared to the following values; ΔNO_3, and consequently the slopes (α and α_{ris}) of NO_3 concentration-flow regressions were positive while HI_N values were consistently negative (SI Fig S5b,e,h).

3.5. Occurrence and distribution of untypical hysteretic patterns

Several events depicted alternative hydro-chemical behavior to the dominant patterns described in section 3.2. Anticlockwise Tu-Q hystereses (negative HI_{Tu}, with accretion pattern too) occur for 16% of recorded events mainly in autumn and spring periods (25% in both May and November; 13% in both April and December) corresponding to rewetting (17%) and recession (19%) phases in terms of hydrological season.

The occurrence of anticlockwise NO_3-Q loops with dilution pattern (negative HI_N and negative slopes) represents 23% of the events and is more frequent during the winter months. Although it is observed all along the year, 81% of these events are occurring during the high flow period (which anyway concentrates the occurrence of events whatever their pattern).

The occurrence of positive NO_3-Q loop (accretion pattern) is rare (2% of the events) and limited to the very beginning of the water year (Fig 3b,e,h), in the early rewetting period.

Finally, the occurrence of clockwise DOC-Q hystereses with accretion pattern (9% of the events) corresponds mainly to winter (60% in January, 62% in high flow period).

The temporal distribution and percentage of each atypical pattern are reported in supplementary material (SI Fig S4).

Figure 2. Distribution by hydrological periods of antecedent conditions (a.: API), event (b. Pev), and stream hydrological response (c. ΔQ, d. ΔTris) and of initial riparian (e) and hillslope (f) groundwater depth in the transects K and G. Histograms represent the mean value and error bar the standard deviation.

Figure 3. Distribution by hydrological periods of a selection of descriptors related to the hydro-chemical stream responses in terms of Turbidity (a,d,g), NO_3 (b,e,h) and DOC (c,f,i) concentrations. Histograms represent the mean value and error bar the standard deviation.

4 Discussion

4.1 Most frequent chemical storm responses from hystereses interpretation

4.1.1 Clockwise Tu-Q hysteresis with accretion pattern

Clockwise hystereses with accretion pattern have been frequently observed elsewhere for turbidity (Asselman, 1999; Lawler et al., 2006; Williams, 1989) and involve (i) an increase of turbidity in storm flow compared to base flow and (ii) a higher turbidity during the rising limb than during the falling limb of the storm hydrograph (Evans and Davies, 1998; Evans et al., 1999). As a proxy of suspended sediments (SS), this increase of turbidity reveals the mobilization of suspended solids. The clockwise pattern suggests a proximal source with possible rapid exhaustion (Sherriff et al., 2016). Thus, the stream bed could be an important source of SS (Fig 4) because of low bed storage of sediments thanks to the protection by riparian vegetation almost all along the stream network in its downstream area (Dupas et al., 2015a; Lefrancois et al., 2007). However, the hypothesis of a hillslope origin is also consistent with the observed Tu-Q pattern as overland flow contributes mostly during the rising limb phase too.

4.1.2 Clockwise NO_3-Q hysteresis with dilution pattern

Storm hysteresis patterns observed for NO_3 are more variable among sites according to the variability of NO_3 sources. Accretion patterns have been reported on agricultural sites (Bowes et al., 2015; Jiang et al., 2010; Dupas et al., 2016; Outram et al. 2016). Dilution patterns are also observed elsewhere but can be dominated by anticlockwise loop (Butturini et al., 2008)

or clockwise as in our case (Lloyd et al., 2016). The shallow groundwater which dominates base flow is the main source of NO_3 as largely demonstrated on this catchment because of this large storage (Aubert et al., 2013a; Molenat et al., 2002; Molenat et al., 2008). Data that support this interpretation are described in Aubert et al. (2013a) showing that upslope groundwater concentration was around 90 mg NO_3/L while downslope groundwater concentration was almost zero. Data presented in Pauwels et al. (2000) highlighted the rapid decrease of NO_3 concentration of the deep groundwater in the fractured layers. The relative decrease of shallow groundwater contribution during the storm is then responsible for the dilution of NO_3. The clockwise direction involves a highest dilution during the falling limb. This may be related to the dominant contribution of riparian denitrified water (Oehler et al., 2007) during this phase, while the overland flow that dominates the rising limb phase may contain more NO_3 (Fig 4).

4.1.3 Anticlockwise DOC-Q hysteresis with accretion pattern

Like for turbidity, the accretion pattern resulting from DOC-richer storm contributors is widely observed in streams (e.g. Inamdar and Mitchell, 2006; McGlynn and McDonnell, 2003). The anticlockwise accretion is not specific to our catchment (Cerro et al., 2014) but clockwise or linear patterns have also been reported (Butturini et al., 2008). The anticlockwise hysteresis involves that contributors during the falling limb are richer in DOC than during the rising limb. Groundwater contains no DOC (concentrations <1mg $C.L^{-1}$) because it is retained in the upper soil layers adsorbed to soil particles as shown by data from piezometer samplings presented in Aubert et al. (2013b). The main sources of DOC during storm have indeed been identified as the riparian wetland soils by Morel et al. (2009) and Lambert et al. (2014) using hydrograph deconvolutions based on various solutes and carbon isotopic signature. Based on

a few events along the year their contribution has been shown dominant during the falling limb (Durand and Juan Torres, 1996).

The most-frequently observed hysteretic patterns for turbidity, NO_3 and DOC concentrations with flow during storms are thus consistent with previous knowledge. Their combination leads to a conceptual scheme of the dominant flow pathway successions over the storm synthesized in Fig 4. Such a conceptual scheme is similar to those proposed e.g. by Rozemeijer and Broers (2007) to explain surface water quality at different discharges with different groundwater mixing ratios at the regional scale.

Figure 4. Sketch of the successive dominant flow paths and related properties regarding their chemical composition. SGW: shallow groundwater; DGW: deep groundwater. Such a succession leads to the typical observed hysteretic patterns: Clockwise Tu-Q with accretion, Clockwise NO3-Q with dilution and Anticlockwise DOC-Q with accretion.

4.2 Interpretation of untypical hysteretic patterns

4.2.1Anticlockwise Tu-Q hystereses

Inversion of the hysteresis direction occurs when falling limb contribution is more turbid than the rising limb contribution. This may be related to mobilization of more distant sediment sources (Fig 5a), *e.g.* further in the hillslope as interpreted for particulate phosphorus (Dupas et al., 2015a; Dupas et al., 2015c) or highly connected poached areas (Sherriff et al., 2016).

4.2.2 Anticlockwise NO_3-Q loops with dilution pattern

Such patterns suggest a less diluted contribution during the falling limb. This lower dilution may be related to (Hypothesis 1) less denitrified riparian wetland water after a period where

soils are unsaturated even in the riparian domain leading to aerobic conditions; or (Hypothesis 2) to higher contribution of shallow groundwater during the falling limb of the hydrograph which is the richest compartment in NO_3 (Fig 5b).

4.2.3 Accretion pattern for NO_3-Q

Such flushing episodes show that for a very few events, the storm flow may be richer in NO_3 than base flow. This can be explained by lower initial conditions, if for instance base flow contribution would be dominated by deep groundwater poorer in NO_3 than the shallower. Another possible mechanism would be the punctual activation of rapid NO_3 transfer from soils (Fig 5a).

4.2.4 Clockwise DOC-Q hystereses with accretion pattern

Such untypical loop suggests that a few events present rising limb contributions that are richer in DOC than falling limb ones. This may be explained by either an exhaustion of the DOC storm sources or a higher contribution of shallow groundwater during the falling limb of the hydrograph that would dilute rapidly DOC concentration from the riparian soils (see Hypothesis 2 above). This last hypothesis is especially possible when it co-occurs with untypical anticlockwise negative NO_3-Q loops as it is observed for 60% of these untypical DOC patterns while all the recorded events with untypical DOC-Q hysteresis still depicted a classical positive and clockwise Tu-Q loop (Fig 5b).

These untypical hysteretic patterns led us to complete the conceptual model of the dominant flow pathway successions (Fig 4) with the alternative successions synthesized in Fig 5.

Figure 5. Sketch of alternative successions of dominant flow paths and related properties regarding their chemical composition. SGW: shallow groundwater; DGW: deep groundwater. Such successions may lead to the untypical observed hysteretic patterns in a) low flow: Anticlockwise Tu-Q with accretion and/or anticlockwise NO_3-Q with accretion; and in b) High flow: Anticlockwise NO_3-Q with dilution and/or Clockwise DOC-Q with accretion.

4.2 Intra annual variability of the storm patterns: dynamics of flow paths connecting sources

The variability of precipitation event between seasons (or months) is relatively low. According to the correlations between stream flow response and groundwater levels (Table S2) and comparing the intra annual variability of those variables (Fig 2) the hydrological storm response is controlled by the shallow groundwater fluctuation as is the base flow (Molenat et al., 2008).

The correlation between turbidity variables and groundwater depths (Table S3) is arguably the consequence of their correlation with flow which controls the transport capacity of the stream (channel source of SS). Alternatively, this correlation could reflect a direct link between SS exports and the extension of areas saturated by groundwater which impact the erosion capacity via the connectivity of hillslope SS sources (Sherriff et al., 2016). When connectivity is maximal in high flow winter period, the hysteretic pattern is stronger (higher HI values) as both sources are combined. In the recession period, when connectivity is minimal due to lower groundwater table location, richness of the mobilized sources is more variable from an event to another leading to this higher variability of turbidity descriptors during spring and summer, and the occurrence of rarer anticlockwise Tu-Q hysteresis. Indeed, at these recession periods because of the combination of less extended saturated areas and occurrence of flashy summer storms associated to intense precipitation events, the surface flowpath responsible for

the highest turbidity events is likely to be hortonian runoff that is sensitive to both the soil cover and the rain event intensity (Dupas et al., 2015a,c). Moreover, erosion risk can be higher in such periods, as it also coincides with seedbed preparation period in Spring, and with maize harvesting Autumn. Finally, rewetting period is critical as it directly follows the phase where the stream may be intermittent and where some material is likely to accumulate until the very first flow events of the water year.

The NO_3 storm response depicts most of really untypical events (accretion pattern) concentrated at the very beginning of the water year, in the rewetting critical phase (October). This phase matches with the minimal groundwater depths. The shallow groundwater contribution is limited because of low gradients along hillslopes so that base flow is dominated by deep groundwater which is poorer in NO_3 as already identified on base flow NO_3 concentration pattern in e.g. (Martin et al., 2004). Furthermore, at this period soils are also re-wetting and this process is likely to re-enhance microbial activity, in particular mineralization producing quickly some nitrate that can be available for transfer to runoff water (Fig 6a). The number of such events is relatively limited and thus, only near continuous monitoring could have been able to capture them. Then, the NO_3 storm response variables emphasized 2 periods that correspond to high and low shallow groundwater levels with less linear behavior and more variable hysteresis in the last one. Hence, groundwater being the main NO_3 storage in the catchment, its seasonal connectivity seems to drive NO_3 dynamics during storm events as during base flow.

The DOC storm response variability can be described only for the first part of the water year unfortunately. All variables except the hysteresis indices depict a continuous decrease along the year suggesting an exhaustion of the storm DOC sources. Such exhaustion has been

emphasized for base flow DOC concentration as well (Humbert et al., 2015) and was already suggested over a succession of 5-6 events in Morel et al. (2009) and Lambert et al. (2014), and is here further supported by the continuous records over the first part of the water year.

Finally, the shallow groundwater seems to drive the dynamics of the flow paths that connect, progressively or abruptly depending of the water year, and transfer each element from its storage compartment to the stream:

(i) Sediments sources from the hillslope are the top of soils, connected via surface runoff on areas saturated by the groundwater. This flow path is intermittent because activated only during rain events. Sediments also originated from the channel bed. When groundwater is high, it supports indirectly high discharge during the storm that results in high transport capacity. When groundwater table decreases, more complex combinations of surface flow paths drive the sediments export.

(ii) Organic carbon sources are located in the upper soil horizons mainly in downslope and riparian areas which are connected to the stream via lateral subsurface flow of groundwater within soils. This flow path is active during rain events (main contributor of the falling limb), but also possibly during base flow in riparian areas.

(iii) Nitrate storage is located in the groundwater which is more continuously connected to the stream but with seasonal fluctuations as well. When the groundwater connectivity is lower (transition periods of autumn and spring) the consistency of this generic pattern is decreased leading to more independence between surface and below ground flows as expressed though untypical patterns.

5 Conclusion

We analyzed the controlling factors of intra-annual variability of the response of stream water composition to storms in order to test the role of shallow groundwater in structuring this seasonal variability at storm level. For that purpose, we proposed a method to characterize storm response of stream water composition using a continuous high frequency data set of multiple parameters by identifying a set of functional indicators. Also, similar functional indicators used in this paper have been used in other studies. Those indicators were based among a large set of descriptors of precipitation input, antecedent and initial discharge and groundwater conditions, and of combined hydro/chemical responses (turbidity, NO_3 and DOC concentrations).

We identified dominant and untypical storm patterns that are interpreted in terms of flow paths successions during storms and related successions of sources mobilization. The seasonal distribution of storm patterns and their features supports the role of groundwater fluctuations as a major control of storm temporal variability. Conditioning the connectivity between sources of sediments, nitrate or organic carbon and the stream, the groundwater ultimately drives the temporal variations of water composition dynamics during storms as it does for base flow stream water composition. For each element, the sources differ in terms of location, size and depletion dynamics.

Acknowledgments

This work was funded by the Agence Nationale de la Recherche via the MOSAIC project and by INRA for the monitoring in the Kervidy-Naizin catchment - ERO AgrHyS. Data are available via http://geowww.agrocampus-ouest.fr/portails/?portail=vidae. The authors also thank all those who helped with the lab work: Béatrice Trinkler, Laurence Carteaux, Yannick Fauvel, Patrice Petitjean, and Armelle Racapé.

References

Asselman, N.E.M., 1999. Suspended sediment dynamics in a large drainage basin: the River Rhine. Hydrological Processes, 13(10): 1437-1450. DOI:10.1002/(sici)1099-1085(199907)13:10<1437::aid-hyp821>3.0.co;2-j

Aubert, A.H. et al., 2013a. Solute transport dynamics in small, shallow groundwater-dominated agricultural catchments: insights from a high-frequency, multisolute 10 yr-long monitoring study. Hydrology and Earth System Sciences, 17(4): 1379-1391. DOI:10.5194/hess-17-1379-2013

Aubert, A.H., Gascuel-Odoux, C., Merot, P., 2013b. Annual hysteresis of water quality: A method to analyse the effect of intra- and inter-annual climatic conditions. Journal of Hydrology, 478: 29-39. DOI:10.1016/j.jhydrol.2012.11.027

Aubert, A.H. et al., 2013c. Clustering flood events from water quality time series using Latent Dirichlet Allocation model. Water Resour. Res., 49(12): 8187-8199. DOI:10.1002/2013wr014086

Bernal, S., Butturini, A., Sabater, F., 2002. Variability of DOC and nitrate responses to storms in a small Mediterranean forested catchment. Hydrol. Earth Syst. Sci., 6(6): 1031-1041. DOI:10.5194/hess-6-1031-2002

Bieroza, M.Z., Heathwaite, A.L., 2015. Seasonal variation in phosphorus concentration–discharge hysteresis inferred from high-frequency in situ monitoring. Journal of Hydrology, 524(0): 333-347. DOI:http://dx.doi.org/10.1016/j.jhydrol.2015.02.036

Blaen, P.J. et al., 2016. Real-time monitoring of nutrients and dissolved organic matter in rivers: Capturing event dynamics, technological opportunities and future directions. Science of the Total Environment, 569–570: 647-660. DOI:http://dx.doi.org/10.1016/j.scitotenv.2016.06.116

Borah, D.K., Bera, M., 2004. Watershed-scale hydrologic and nonpoint-source pollution models: Review of applications. Transactions of the Asae, 47(3): 789-803.

Bowes, M.J., House, W.A., Hodgkinson, R.A., Leach, D.V., 2005. Phosphorus–discharge hysteresis during storm events along a river catchment: the River Swale, UK. Water Research, 39(5): 751-762. DOI:http://dx.doi.org/10.1016/j.watres.2004.11.027

Bowes, M.J. et al., 2015. Characterising phosphorus and nitrate inputs to a rural river using high-frequency concentration–flow relationships. Science of the Total Environment, 511(0): 608-620. DOI:http://dx.doi.org/10.1016/j.scitotenv.2014.12.086

Butturini, A., Alvarez, M., Bernal, S., Vazquez, E., Sabater, F., 2008. Diversity and temporal sequences of forms of DOC and NO3-discharge responses in an intermittent stream: Predictable or random succession? J. Geophys. Res.-Biogeosci., 113(G3). DOI:10.1029/2008jg000721

Cerro, I., Sanchez-Perez, J.M., Ruiz-Romera, E., Antigüedad, I., 2014. Variability of particulate (SS, POC) and dissolved (DOC, NO3) matter during storm events in the Alegria agricultural watershed. Hydrological Processes, 28(5): 2855-2867. DOI:10.1002/hyp.9850

Dupas, R., Gascuel-Odoux, C., Gilliet, N., Grimaldi, C., Gruau, G., 2015a. Distinct export dynamics for dissolved and particulate phosphorus reveal independent transport mechanisms in an arable headwater catchment. Hydrological Processes, 29: 3162–3178. DOI:10.1002/hyp.10432

Dupas, R., Jomaa, S., Musolff, A., Borchardt, D., Rode, M., 2016. Disentangling the influence of hydroclimatic patterns and agricultural management on river nitrate dynamics from sub-hourly to decadal time scales. Science of the Total Environment, 571: 791-800. DOI:http://dx.doi.org/10.1016/j.scitotenv.2016.07.053

Dupas, R. et al., 2015b. Identifying seasonal patterns of phosphorus storm dynamics with dynamic time warping. Water Resour. Res., 51(11): 8868-8882. DOI:10.1002/2015wr017338

Durand, P., Juan Torres, J.L., 1996. Solute transfer in agricultural catchments: the interest and limits of mixing models. Journal of Hydrology, 181(1): 1-22. DOI:http://dx.doi.org/10.1016/0022-1694(95)02922-2

Evans, C., Davies, T.D., 1998. Causes of concentration/discharge hysteresis and its potential as a tool for analysis of episode hydrochemistry. Water Resour. Res., 34(1): 129-137. DOI:10.1029/97wr01881

Evans, C., Davies, T.D., Murdoch, P.S., 1999. Component flow processes at four streams in the Catskill Mountains, New York, analysed using episodic concentration/discharge relationships. Hydrological Processes, 13(4): 563-575.

Faucheux, M., Fovet, O., 2014. Mesures in situ et à haute fréquence de la chimie d'un cours d'eau par spectrophotométrie UV-visible. Le Cahier Technique de l'INRA, 82(2): 1-15.

Feinson, L.S., Gibs, J., Imbrigiotta, T.E., Garrett, J.D., 2016. Effects of land use and sample location on Nitrate-stream flow hysteresis descriptors during storm events. JAWRA Journal of the American Water Resources Association, 52(6): 1493-1508. DOI:10.1111/1752-1688.12477

Gascuel-Odoux, C., Aurousseau, P., Durand, P., Ruiz, L., Molenat, J., 2010. The role of climate on inter-annual variation in stream nitrate fluxes and concentrations. Science of the Total Environment, 408(23): 5657-5666. DOI:10.1016/j.scitotenv.2009.05.003

Halliday, S.J. et al., 2013. Upland streamwater nitrate dynamics across decadal to sub-daily timescales: a case study of Plynlimon, Wales. Biogeosciences, 10(12): 8013-8038. DOI:10.5194/bg-10-8013-2013

Hill, A.R., 1993. Base cation chemistry of storm runoff in a forested headwater wetland. Water Resour. Res., 29(8): 2663-2673. DOI:10.1029/93wr00758

House, W.A., Warwick, M.S., 1998. Hysteresis of the solute concentration/discharge relationship in rivers during storms. Water Research, 32(8): 2279-2290. DOI:http://dx.doi.org/10.1016/S0043-1354(97)00473-9

Humbert, G., Jaffrezic, A., Fovet, O., Gruau, G., Durand, P., 2015. Dry-season length and runoff control annual variability in stream DOC dynamics in a small, shallow groundwater-dominated agricultural watershed. Water Resour. Res., 51(10): 7860-7877. DOI:10.1002/2015wr017336

Inamdar, S.P., Mitchell, M.J., 2006. Hydrologic and topographic controls on storm-event exports of dissolved organic carbon (DOC) and nitrate across catchment scales. Water Resour. Res., 42(3). DOI:W03421 10.1029/2005wr004212

Jeong, J.J. et al., 2012. Differential storm responses of dissolved and particulate organic carbon in a mountainous headwater stream, investigated by high-frequency, in situ optical measurements. J. Geophys. Res.-Biogeosci., 117. DOI:G03013 10.1029/2012jg001999

Jiang, R. et al., 2010. Hydrological process controls on nitrogen export during storm events in an agricultural watershed. Soil Science and Plant Nutrition, 56(1): 72-85. DOI:10.1111/j.1747-0765.2010.00456.x

Johnson, F.A., East, J.W., 1982. Cyclical relationships between river discharge and chemical concentration during flood events. Journal of Hydrology, 57(1): 93-106. DOI:http://dx.doi.org/10.1016/0022-1694(82)90105-6

Kirchner, J.W., Feng, X., Neal, C., Robson, A.J., 2004. The fine structure of water-quality dynamics: the (high-frequency) wave of the future. Hydrological Processes, 18(7): 1353-1359. DOI:10.1002/hyp.5537

Ladouche, B. et al., 2001. Hydrograph separation using isotopic, chemical and hydrological approaches (Strengbach catchment, France). Journal of Hydrology, 242(3-4): 255-274. DOI:10.1016/s0022-1694(00)00391-7

Lambert, T. et al., 2013. Hydrologically driven seasonal changes in the sources and production mechanisms of dissolved organic carbon in a small lowland catchment. Water Resour. Res., 49(9): 5792-5803. DOI:10.1002/wrcr.20466

Lambert, T. et al., 2014. DOC sources and DOC transport pathways in a small headwater catchment as revealed by carbon isotope fluctuation during storm events. Biogeosciences, 11(11): 3043-3056. DOI:10.5194/bg-11-3043-2014

Lawler, D.M., Petts, G.E., Foster, I.D.L., Harper, S., 2006. Turbidity dynamics during spring storm events in an urban headwater river system: The Upper Tame, West Midlands, UK. Science of the Total Environment, 360(1–3): 109-126. DOI:http://dx.doi.org/10.1016/j.scitotenv.2005.08.032

Lefrancois, J., Grimaldi, C., Gascuel-Odoux, C., Gilliet, N., 2007. Suspended sediment and discharge relationships to identify bank degradation as a main sediment source on small agricultural catchments. Hydrological Processes, 21(21): 2923-2933. DOI:10.1002/hyp.6509

Lloyd, C.E.M., Freer, J.E., Johnes, P.J., Collins, A.L., 2016a. Technical Note: Testing an improved index for analysing storm discharge–concentration hysteresis. Hydrol. Earth Syst. Sci., 20(2): 625-632. DOI:10.5194/hess-20-625-2016

Lloyd, C.E.M., Freer, J.E., Johnes, P.J., Collins, A.L., 2016b. Using hysteresis analysis of high-resolution water quality monitoring data, including uncertainty, to infer controls on nutrient and sediment transfer in catchments. Science of the Total Environment, 543, Part A: 388-404. DOI:http://dx.doi.org/10.1016/j.scitotenv.2015.11.028

Martin, C. et al., 2004. Seasonal and interannual variations of nitrate and chloride in stream waters related to spatial and temporal patterns of groundwater concentrations in agricultural catchments. Hydrological Processes, 18(7): 1237-1254. DOI:10.1002/hyp.1395

McGlynn, B.L., McDonnell, J.J., 2003. Role of discrete landscape units in controlling catchment dissolved organic carbon dynamics. Water Resour. Res., 39(4). DOI:1090 10.1029/2002wr001525

Molenat, J., Durand, P., Gascuel-Odoux, C., Davy, P., Gruau, G., 2002. Mechanisms of nitrate transfer from soil to stream in an agricultural watershed of French Brittany. Water Air and Soil Pollution, 133(1-4): 161-183. DOI:10.1023/a:1012903626192

Molenat, J., Gascuel-Odoux, C., Ruiz, L., Gruau, G., 2008. Role of water table dynamics on stream nitrate export and concentration. in agricultural headwater catchment (France). Journal of Hydrology, 348(3-4): 363-378. DOI:10.1016/j.jhydrol.2007.10.005

Morel, B., Durand, P., Jaffrezic, A., Gruau, G., Molenat, J., 2009. Sources of dissolved organic carbon during stormflow in a headwater agricultural catchment. Hydrological Processes, 23(20): 2888-2901. DOI:10.1002/hyp.7379

Ockenden, M.C. et al., 2016. Changing climate and nutrient transfers: Evidence from high temporal resolution concentration-flow dynamics in headwater catchments. Science of the Total Environment, 548–549: 325-339. DOI:http://dx.doi.org/10.1016/j.scitotenv.2015.12.086

Oehler, F., Bordenave, P., Durand, P., 2007. Variations of denitritication in a farming catchment area. Agriculture Ecosystems & Environment, 120(2-4): 313-324. DOI:10.1016/j.agee.2006.10.007

Outram, F.N., Cooper, R.J., Sünnenberg, G., Hiscock, K.M., and Lovett, A.A., 2016. Antecedent conditions, hydrological connectivity and anthropogenic inputs: Factors affecting nitrate and phosphorus transfers to agricultural headwater streams. Science of The Total Environment, 545–546:184-199, DOI: 10.1016/j.scitotenv.2015.12.025.

Pauwels, H., Foucher, J-C., Kloppmann, W., 2000. Denitrification and mixing in a schist aquifer: influence on water chemistry and isotopes. Chemical Geology 168: 307–324.

Penna, D. et al., 2015. Seasonal changes in runoff generation in a small forested mountain catchment. Hydrological Processes, 29(8): 2027-2042. DOI:10.1002/hyp.10347

R Development Core Team, 2008. R: A language and environment for statistical computing. R Foundation for Statistical Computing, Vienna, Austria. URL http://www.R-project.org.

Rode, M. et al., 2016. Sensors in the Stream: The high-frequency wave of the present. Environmental Science & Technology, 50(19): 10297-10307. DOI:10.1021/acs.est.6b02155

Rozemeijer, J.C., and Broers, H.P., 2007. The groundwater contribution to surface water contamination in a region with intensive agricultural land use (Noord-Brabant, The Netherlands). Environmental Pollution, 148(3): 695-706, https://doi.org/10.1016/j.envpol.2007.01.028.

Ruhala, S.S., Zarnetske, J.P., 2017. Using in-situ optical sensors to study dissolved organic carbon dynamics of streams and watersheds: A review. Science of the Total Environment, 575: 713-723. DOI: 10.1016/j.scitotenv.2016.09.113

Scilab Enterprises, 2012. Scilab: Free and Open Source software for numerical computation (OS, Version 5.XX) [Software]. Available from: http://www.scilab.org.Sherriff, S.C. et al., 2016. Storm event suspended sediment-discharge hysteresis and controls in agricultural watersheds: Implications for watershed scale sediment management. Environmental Science & Technology, 50(4): 1769-1778. DOI:10.1021/acs.est.5b04573

van Geer, F.C., Kronvang, B., Broers, H.P., 2016. High-resolution monitoring of nutrients in groundwater and surface waters: process understanding, quantification of loads and concentrations, and management applications. Hydrol. Earth Syst. Sci., 20(9): 3619-3629. DOI:10.5194/hess-20-3619-2016

Vidon, P., Allan, C., Burns, D., Duval, T. P., Gurwick, N., Inamdar, S., Lowrance, R., Okay, J., Scott, D. and Sebestyen, S., 2010. Hot Spots and Hot Moments in Riparian Zones: Potential for Improved Water Quality Management. Journal of the American Water Resources Association, 46(2):278-298. DOI: 10.1111/j.1752-1688.2010.00420.x

Wade, A.J. et al., 2012. Hydrochemical processes in lowland rivers: insights from in situ, high-resolution monitoring. Hydrol. Earth Syst. Sci., 16(11): 4323-4342. DOI:10.5194/hess-16-4323-2012

Williams, G.P., 1989. Sediment concentration versus water discharge during single hydrologic events in Rivers. Journal of Hydrology, 111(1-4): 89-106. DOI:10.1016/0022-1694(89)90254-0.

Table 1. General statistics of descriptors related to event and anterior and initial conditions. P_{24h} and Pev are antecedent and event precipitations, API is the antecedent precipitation index for 4 days, variables denoted Xi are values at initial time of storm hydrograph of discharge (Q), groundwater level on transect K and G at upslope (K/Gu), midslope (Gm) and downslope (K/Gd) locations, turbidity (Tu) and concentration in Nitrate (NO_3) and Dissolved Organic Carbon (DOC).

	P_{24h} (mm)	Pev (mm)	API (mm)	Qi (L/s)	Kdi (m)	Kui (m)	Gdi (m)	Gmi (m)	Gui (m)	Tui (FTU)	NO_3i (mg/L)	DOCi (mg/l)
Std Dev	8.2	8.1	13.5	149.8	0.308	0.924	0.326	0.325	1.251	18.5	10.3	2.6
Mean	**6.1**	**10.3**	**15.2**	**137.6**	**-0.079**	**-1.472**	**-0.136**	**-0.324**	**-1.151**	**13.0**	**60.5**	**6.5**
Max	50.5	47.0	64.3	1202.3	0.081	0.004	0.111	0.077	0.008	211.0	78.5	15.5
90th centile	15.5	21.8	32.4	332.6	0.050	-0.293	0.097	-0.030	-0.038	23.6	73.4	10.2
3rd quartile	8.5	13.0	20.9	227.1	0.039	-0.648	0.064	-0.117	-0.098	15.0	68.0	7.7
Median	**3.5**	**8.0**	**11.6**	**80.6**	**0.025**	**-1.524**	**-0.044**	**-0.297**	**-0.692**	**9.0**	**62.6**	**6.1**
1rst quartile	0.5	5.0	5.4	28.0	-0.073	-2.110	-0.206	-0.417	-1.964	6.0	52.8	4.4
10th centile	0.0	3.0	2.4	10.0	-0.192	-2.675	-0.409	-0.479	-2.957	4.0	47.0	3.9
Min	0.0	0.0	0.0	0.0	-2.279	-3.520	-2.390	-2.413	-5.029	1.0	17.8	2.5
n	*169*	*169*	*177*	*169*	*169*	*158*	*169*	*169*	*169*	*145*	*140*	*71*

Table 2. General statistics of descriptors related to event response based on single time series. ΔTris is the duration of rising limb of the hydrograph, ΔQ the amplitude of discharge variation, ΔKd,u and ΔGd,m,u are amplitude of groundwater levels variations on transects K and G respectively, and at upslope (u), Midslope (m) and downslope (d) locations, ΔTu is the amplitude of turbidity, ΔNO_3 the amplitude of nitrate concentration, and ΔDOC the amplitude of dissolved organic carbon concentration.

	ΔTris (h)	ΔQ (L/s)	ΔKd (m)	ΔKu (m)	ΔGd (m)	ΔGm (m)	ΔGu (m)	ΔTu (FTU)	ΔNO_3 (mg/L)	ΔDOC (mg/l)
Std Dev	3.9	225	0.069	0.224	0.130	0.305	0.179	334	12.1	4.0
Mean	**7.7**	**161**	**0.069**	**0.116**	**0.087**	**0.176**	**0.107**	**194**	**-17.5**	**5.0**
Max	20.0	1178	0.289	1.571	1.165	1.642	1.376	1990	19.6	13.4
90th percentile	12.4	368	0.156	0.215	0.230	0.581	0.242	517	-3.7	10.2
75th percentile	10.1	187	0.098	0.133	0.121	0.180	0.105	220	-9.7	8.2
Median	**7.7**	**79**	**0.042**	**0.046**	**0.043**	**0.049**	**0.048**	**73**	**-15.1**	**4.2**
25th percentile	4.7	30	0.021	0.024	0.017	0.015	0.024	30	-26.1	2.3
10th percentile	3.0	14	0.007	0.014	0.003	0.003	0.014	15	-35.2	1.0
Min	0.2	6	0.001	0.006	0.001	0.000	0.005	3	-45.2	-4.6
n	*168*	*168*	*73*	*57*	*136*	*150*	*96*	*143*	*137*	*67*

Table 3. General statistics of descriptors related to hydro-chemical event response based on coupled time series. α Tu/NO_3/DOC is the slope of the linear regression between turbidity/nitrate concentration/dissolved organic carbon concentration and discharge, R^2Tu/NO_3/DOC is the corresponding determination coefficient, and α_{ris}Tu/NO_3/DOC the slope of similar regression using only data from the rising limb of the hydrograph, $HI_{Tu/N/C}$ (k) are the Hysteresis Indices computed from the relationship between turbidity/nitrate concentration/dissolved organic carbon concentration and Discharge, for k=25, 50 and 75 % of the maximal discharge value reached during the event.

	αTu	R^2 Tu	α_{ris}Tu	$HI_{Tu}(25)$	$HI_{Tu}(50)$	$HI_{Tu}(75)$	α NO_3	R^2 NO_3	α_{ris} NO_3	$HI_N(25)$	$HI_N(50)$	$HI_N(75)$	α DOC	R^2DOC	α_{ris}DOC	$HI_C(25)$	$HI_C(50)$	$HI_C(75)$
Std Dev	0.23	0.26	0.26	0.22	0.26	0.32	0.25	0.26	0.27	0.27	0.29	0.24	0.48	0.35	0.45	0.79	0.37	0.30
Mean	**0.48**	**0.50**	**0.56**	**0.18**	**0.27**	**0.32**	**-0.82**	**0.76**	**-0.74**	**0.09**	**0.13**	**0.13**	**0.62**	**0.55**	**0.55**	**-0.23**	**-0.29**	**-0.29**
Max	1.29	0.95	1.04	0.88	0.85	0.89	0.29	0.99	0.53	0.78	0.90	0.92	1.45	0.99	1.89	0.62	0.53	0.53
90th percentile	0.77	0.83	0.90	0.45	0.69	0.75	-0.52	0.97	-0.40	0.41	0.45	0.40	1.03	0.92	0.90	0.17	0.19	0.14
75th percentile	0.63	0.72	0.78	0.27	0.42	0.57	-0.73	0.94	-0.67	0.23	0.27	0.27	0.93	0.82	0.81	0.00	-0.09	-0.09
Median	**0.49**	**0.52**	**0.54**	**0.13**	**0.21**	**0.32**	**-0.88**	**0.88**	**-0.83**	**0.11**	**0.14**	**0.13**	**0.81**	**0.67**	**0.68**	**-0.15**	**-0.31**	**-0.32**
25th percentile	0.35	0.32	0.37	0.06	0.09	0.09	-0.99	0.64	-0.93	-0.03	0.01	-0.01	0.32	0.15	0.35	-0.32	-0.43	-0.48
10th percentile	0.19	0.10	0.23	0.01	0.01	-0.06	-1.06	0.35	-0.97	-0.13	-0.15	-0.13	-0.01	0.02	0.00	-0.42	-0.75	-0.63
Min	-0.36	0.00	-0.25	-0.65	-0.36	-0.50	-1.36	0.00	-1.00	-0.94	-0.69	-0.53	-1.52	0.00	-0.78	-5.15	-1.40	-0.89
n	*144*	*144*	*143*	*109*	*130*	*139*	*138*	*138*	*138*	*104*	*125*	*135*	*62*	*62*	*62*	*46*	*58*	*61*

Figure1

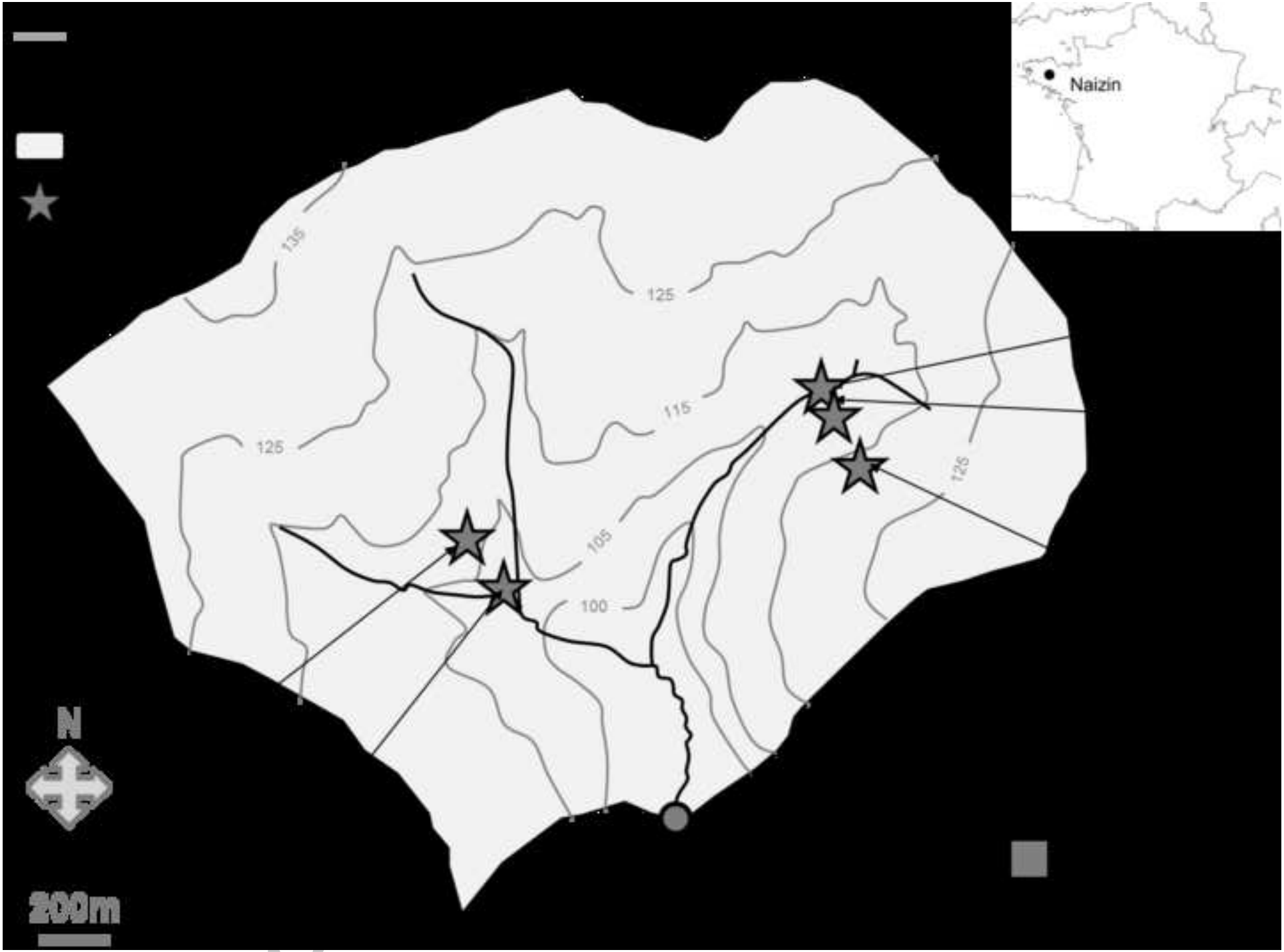

Figure2

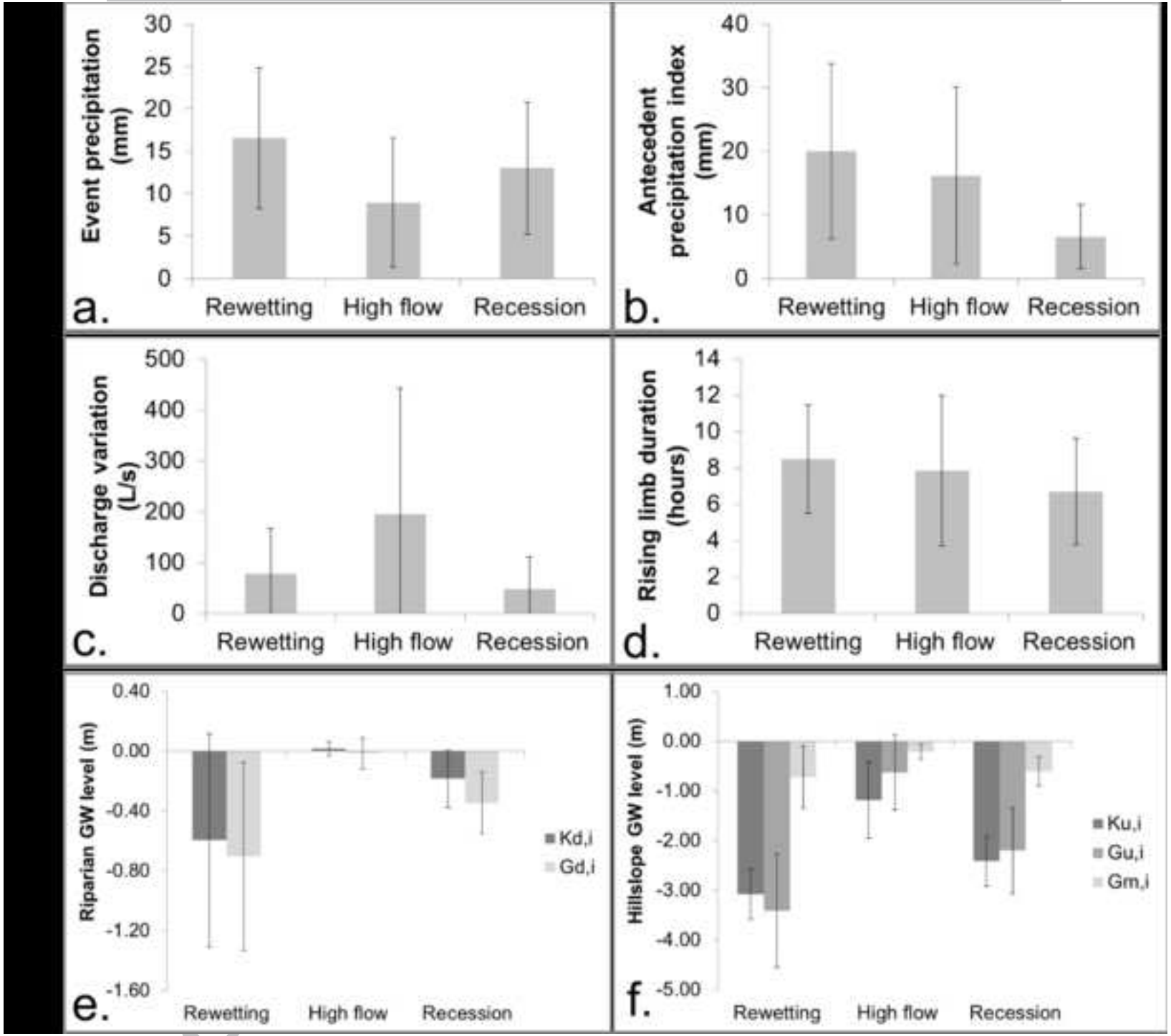

Figure3

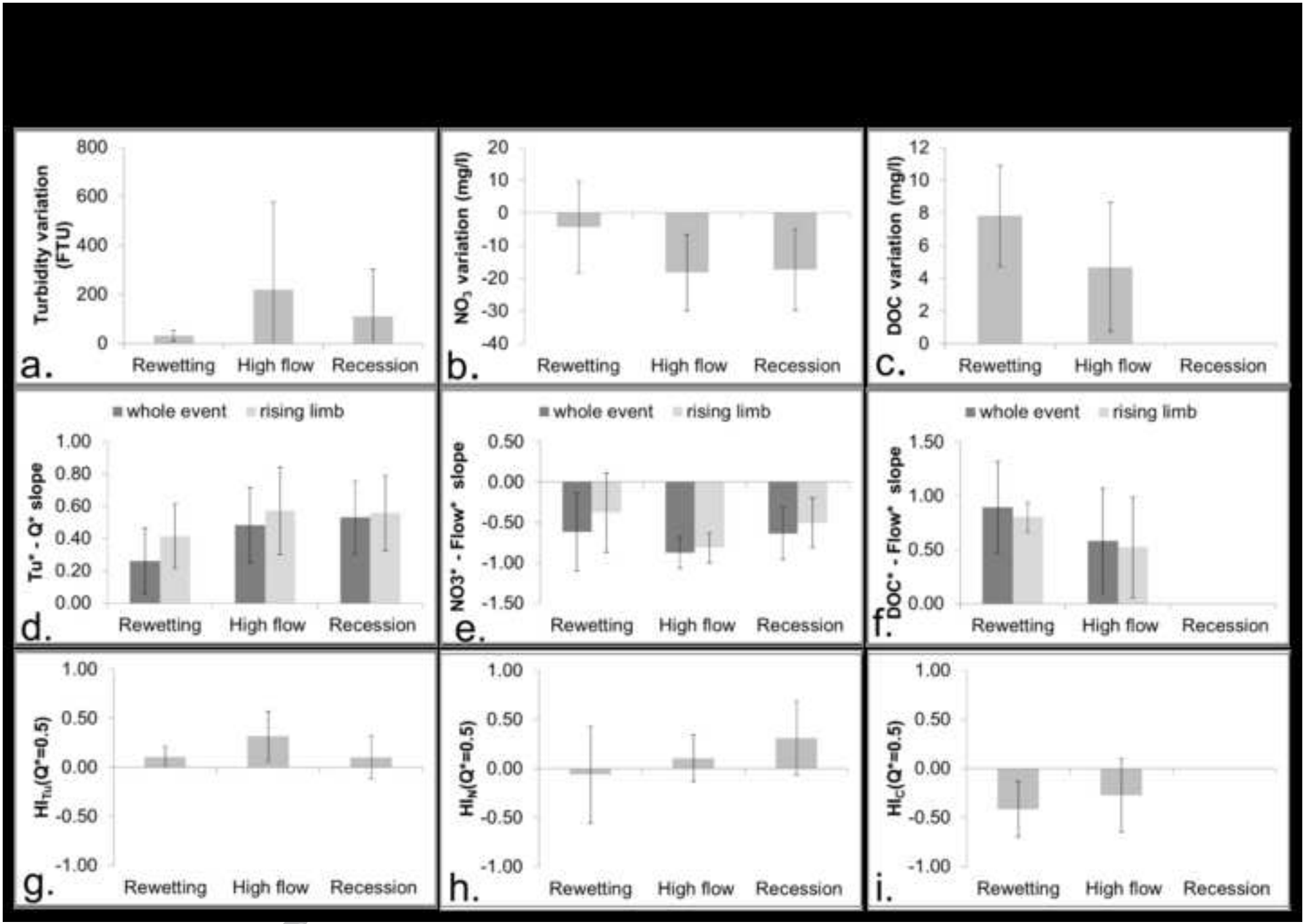

Figure4

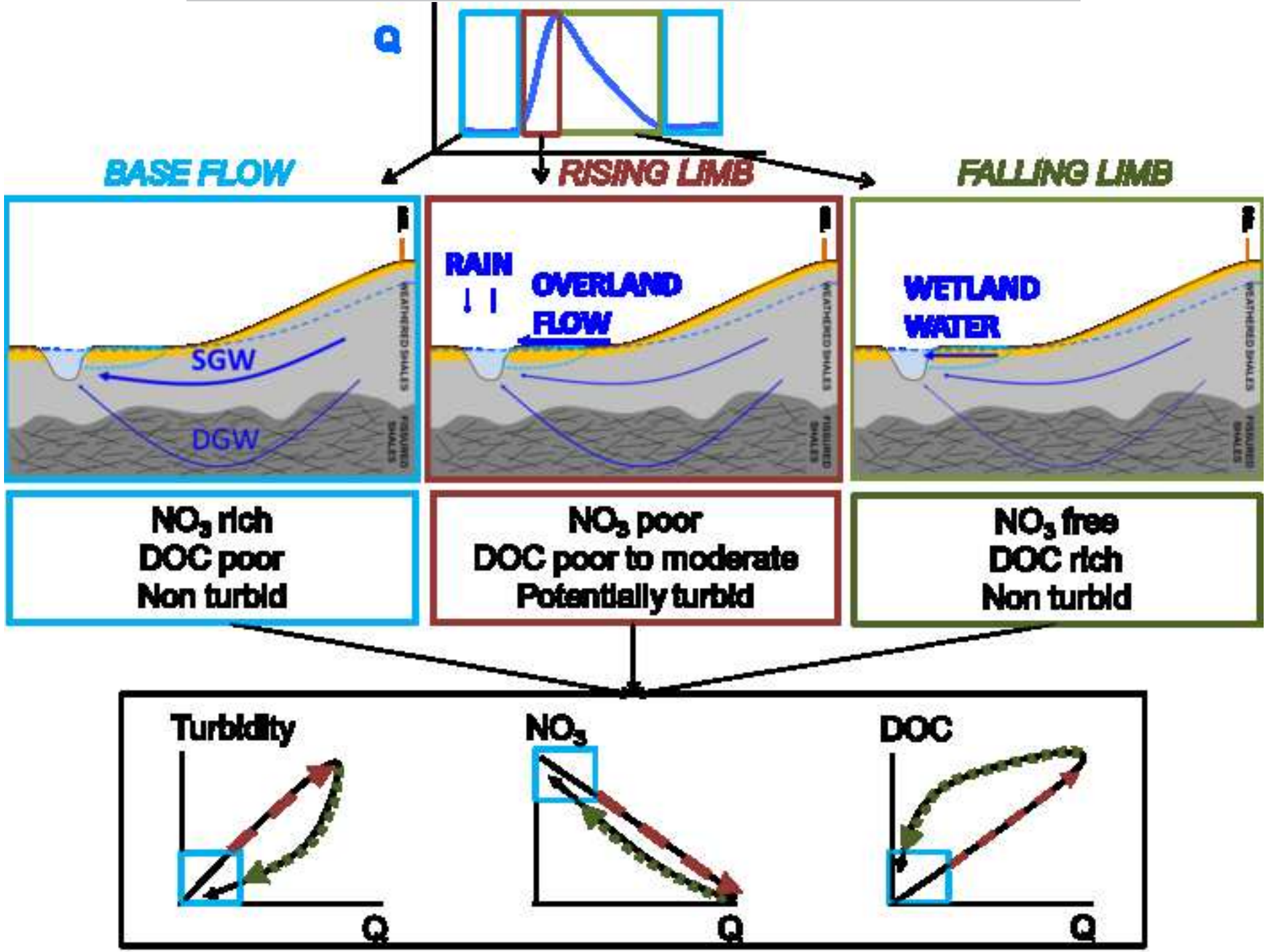

Figure5

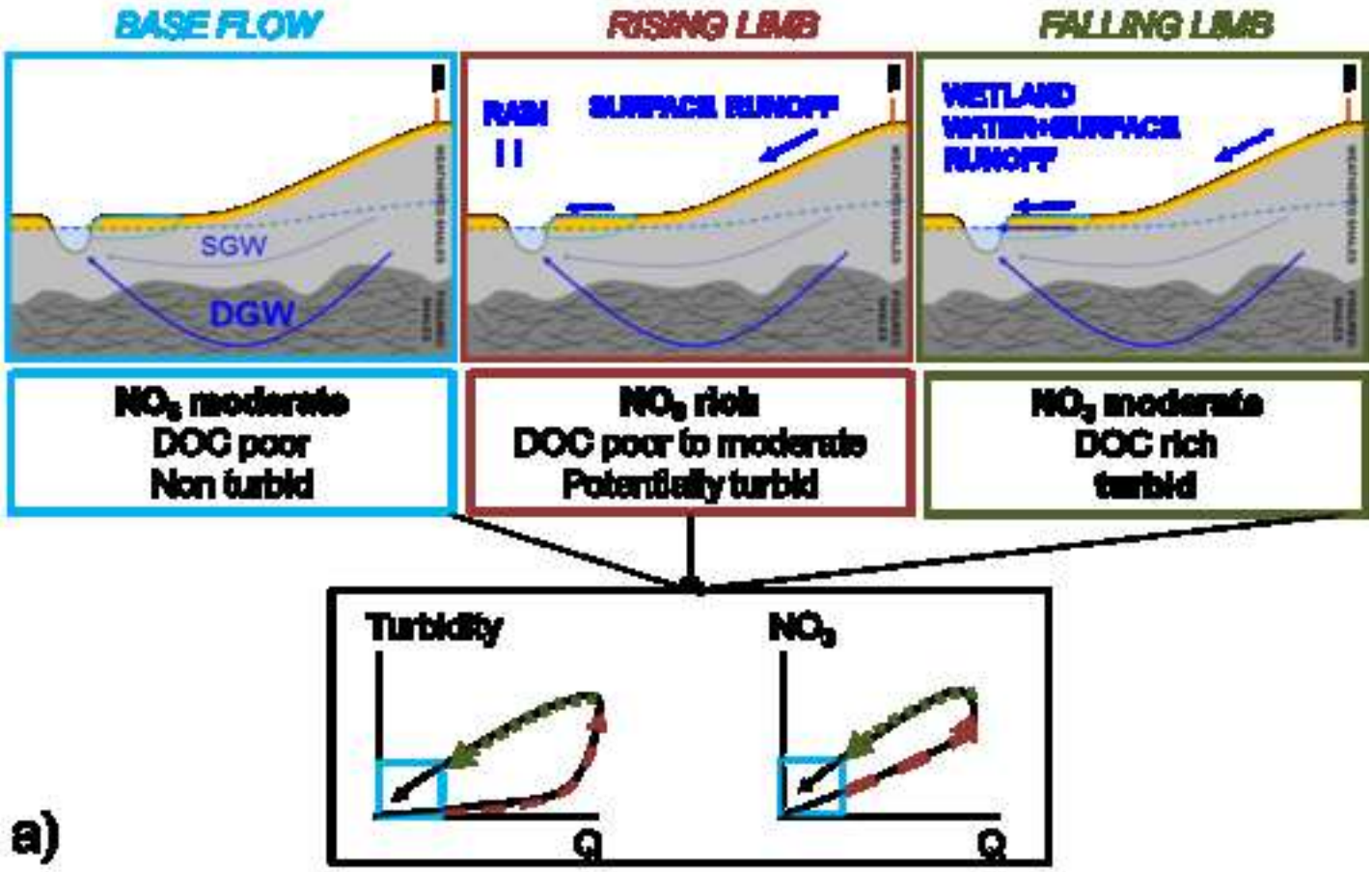

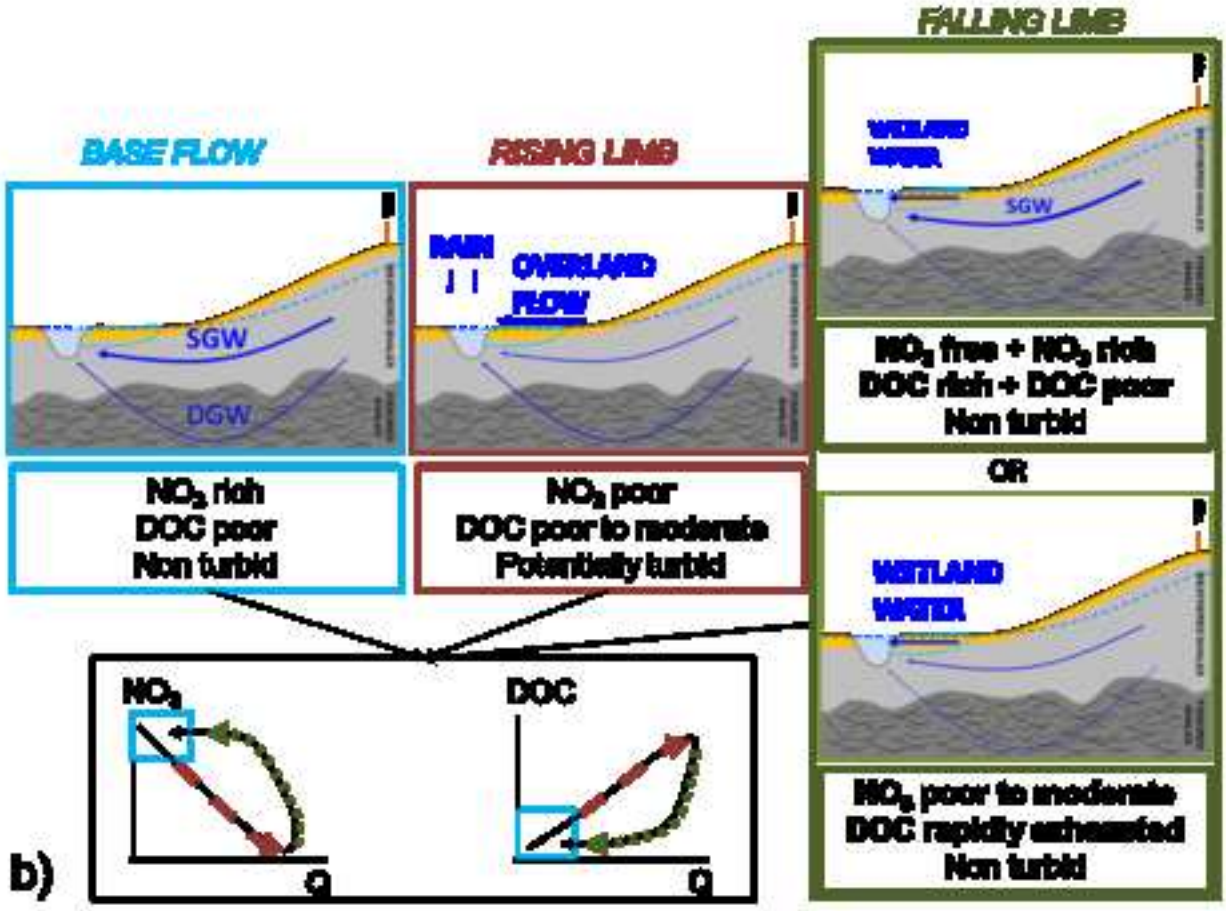

Highlights

- Storms stream flow, turbidity, NO_3 and DOC concentrations and groundwater levels were described
- A set of functional descriptors was proposed to identify and interpret storm patterns
- Groundwater dynamics control seasonality of storm responses via sources connectivity